https://doi.org/10.1016/j.jclepro.2022.134550

Valorization of Macro Fibers Recycled from Decommissioned Turbine Blades as Discrete Reinforcement in Concrete

Guang-Ti Xu[1], Ming-Jie Liu[1], Yu XIANG[2*] and Bing FU[1, 3*]

1. School of Mechanics and Construction Engineering, Jinan University, Guangzhou 510632, China

2. Department of Civil and Environmental Engineering, The Hong Kong Polytechnic University, Hong Kong, China

3. MOE Key Lab of Disaster Forecast and Control in Engineering, Jinan University, Guangzhou 510632, China

ABSTRACT

The extensive use of glass fiber-reinforced polymer (GFRP) composites has inevitably resulted in a large amount of FRP waste, posing a significant environmental threat. A recent study performed by the authors' group of the present study pioneered a new mechanical method of recycling GFRP wind turbine blades into macro fibers, in which the macro fibers characterized by a fixed-length have been produced using a manual process of low efficiency and high cost, making it impossible for use in a practical application. In the present study, a shredding machine has been therefore used to efficiently process waste GFRP wind turbine blades into macro fibers of hybrid lengths lesser than 100 millimeters for being incorporated into concrete. A series of tests were carried out to investigate the properties of the resulting concrete, and the test results of beam specimens were then analyzed using a twice inverse analysis approach. The results of compression tests and four-point bending tests showed that the incorporation of recycled macro fibers led to a slump loss of 54%, a compressive strength reduction of 14.07%, a flexural strength improvement of 37.85% and a significant flexural toughness enhancement of 36.8 times at a fiber volume ratio of 2.5%, as compared to those of plain concrete. The direct-tensile strength and the corresponding tensile strain obtained by a twice inverse analysis approach were about 2.26 MPa and 134 με, respectively, as predicted by the inverse analysis based on flexural load-deflection curves. The macro fibers processed using a shredding machine are feasible for enhancing the performance of the resulting concrete, and can be economic-efficiently used for industrial scale applications.

Keywords: Fiber-reinforced concrete (FRC); Fiber-reinforced polymer (FRP); Recycled; Macro fibers; concrete.

* Corresponding Author:
Dr. Yu XIANG, Department of Civil and Environmental Engineering, The Hong Kong Polytechnic University, Hong Kong, China. Email: cee.yu.xiang@polyu.edu.hk.
Prof. Bing FU, School of Mechanics and Construction Engineering, Jinan University, Guangzhou 510632, China. Email: fubing@jnu.edu.cn.

1. INTRODUCTION

Climate change is the most pressing issue facing the Blue Planet today (Passarelli et al. 2021). Climate change refers to complex shifts in the climate system, including global warming, sea level rise, water scarcity, flooding and other extreme weather events (IPCC 2021). The main driver of these changes is heat-trapping greenhouse gases (GHGs) released from human activities, e.g., industry, transport and building (IPCC 2021; Pierrehumbert 2019). To tackle the planetary crisis, 193 countries have joined the Paris Agreement (United Nations 2015) and are working together to limit the temperature increase to 1.5°C above pre-industrial levels, which requires global greenhouse gas emissions [often transferred to carbon dioxide equivalents (CO_{2e}) and referred to as carbon emissions] to reach net-zero before 2050.

In light of the goal of achieving net-zero emissions by 2050, many parties to the Paris Agreement have established their road maps. For instance, the United States recently released its long-term strategy to reach this goal (U.S. Department of State and U.S. Executive Office of the President 2021), which relies on five key transformations: (1) decarbonize electricity; (2) electrify end uses and switch to other clean fuels; (3) cut energy waste; (4) reduce methane and other non-CO_2 emissions; and (5) scale up CO_2 removal. Pathways for all sectors of the economy are suggested in the Long-Term Strategy of the United States (U.S. Department of State and U.S. Executive Office of the President 2021), e.g., decarbonizing electricity for the electricity sector and scaling up material efficiency for the industrial sector. Decarbonizing electricity refers to the use of renewable generation, e.g., solar and wind, to replace coal-fired generation, whereas scale-up of material efficiency incorporates structural changes in manufacturing that include product recycling and reuse, material substitution, and demand reduction (U.S. Department of State and U.S. Executive Office of the President 2021). Similar energy transmission strategies are also adopted by other parties to the Paris Agreement, e.g., the United Kingdom (U.K. Department for Business, Energy & Industrial Strategy 2021) and Hong Kong Special Administration Region of China (Hong Kong Special Administrative Region 2021). Under these policy-driven actions, 93.6 GW of new wind power capacity was added worldwide in 2021, bringing the cumulative installed wind capacity to 837 GW with a yearly growth of 12.4%. Half of this capacity addition was commissioned in China (47.6 GW); the United States ranked the second most important contributor with a record of 12.7 GW (GWEW 2022). Based on the current growth rate, Global Wind Energy Council (GWEW) expected that 557 GW of new capacity will be added worldwide from 2022 to 2026, equaling more than 110 GW of new installations each year (GWEW 2022). However, to meeting the net-zero 2050 goal (Bouckaert et al. 2021), the annual new installations needs to quadruple to nearly 390 GW during 2022 to 2030 (IEA 2021). As a result, an enormous expansion of on- and off-shore wind turbines is expected to happen in the coming few years.

Fiber-reinforced polymer (FRP) composites are lightweight, high-strength, fatigue-resistant materials (Hollaway 2010), which enable wind turbines with larger blades and thus higher efficiency to be built. Therefore, a modern wind turbine is composed of four components: a foundation made from concrete; a tower made from steel or concrete; a nacelle made mainly from steel and copper; and three blades made from 93% of FRPs (Liu and Barlow 2017). The fast-growing wind power capacity, in conjunction with the "political correctness" of utilizing FRPs to substitute steel and aluminum to improve material efficiency (U.S. Department of State and U.S. Executive Office of the President 2021) will inevitably boost the market of FRPs from 2022 to 2030. Considering an estimated blade material consumption of 12 to 15 tonnes per MW of wind power capacity (Jensen and Skelton 2018) and an estimated lifespan of 20 years of wind turbines (Nagle et al. 2020), it is foreseeable that, from 2042 to 2050, there are annually 4.4 to 5.4 million tonnes of FRPs must be disposed of. However, because of the non-biodegradable nature of FRPs, these decommissioned wind turbines will certainly pose immense pressure on the global environment (Asokan et al. 2009).

Nowadays, FRP waste is normally processed via landfilling, incineration and recycling. Among them, landfilling is a simple and economical method, but it faces higher tax rate and tighter environmental policy. For instance, the amount of waste for landfilling has been reduced by European Commission, whereas, in Germany, landfilling is prohibited (Jacob 2011). Incineration is a thermal treatment method used to reduce the volume of waste requiring final disposal, which allows energy recovery from the waste (Pickering 2006). However, the high toxic emissions associated with FRP incineration usually leads to high cost and environmental challenges (Correia et al. 2011). The above two methods pose great challenges to land resources and atmospheric resources, creating a huge obstacle to the material efficiency strategy (U.S. Department of State and U.S. Executive Office of the President 2021). By contrast, recycling is a more environmental-friendly and sustainable way of dealing with FRP waste.

Recycling of FRP waste includes thermal, mechanical and chemical techniques (Pickering 2006; Yang et al. 2012; Job 2013; Oliveux et al. 2015; Scaffaro et al. 2021; Colombo et al. 2022; Goncalves et al. 2022). Regarding thermal techniques, their applications have reached an industrial scale, e.g., pyrolysis, a technic to decompose FRP waste at various temperatures (300 to 900°C) in the absence of oxygen for recycling fibers, has been implemented by several companies [ELG Carbon Fiber Ltd. (ELGCF) in the UK; Adherent Technologies Inc. (ATI) in the US] for recycling waste CFRP. However, thermal technics have been proven to weaken glass fibers when pyrolyzed at high temperatures. Similar problems also exist in the chemical recycling of FRP waste, and the cost of chemical recycling is too expensive in relative to glass fibers themselves. Mechanical recycling technics, including shredding, grinding, screening, etc., are more economically attractive as compared to thermal and chemical technics. The waste after being treated by mechanical recycling technics is generally used as fillers, aggregates, or reinforcements of construction materials (Yazdanbakhsh et al. 2014; Ribeiro et al. 2015). For instance, pulverized Glass-FRP (GFRP) waste powder was used as a filler for concrete (Tittarelli et al. 2010; Asokan 2009; Correia 2011), but resulted in a reduction of more than 50% in the compressive strength of concrete. Short cylindrical GFRP particles were used to substitute coarse aggregate in concrete (Shahria Alam et al. 2013; Yazdanbakhsh et al. 2016), however, the recycled GFRP aggregate was found detrimental to the mechanical properties of concrete. Singh et al. (2022) examined the suitability of using mechanically shredded GFRP and Carbon-FPR (CFRP) wastes to produce pervious concrete. The results of the lifecycle assessment indicate that a pervious concrete pavement containing recycled GFPR and CFRP wastes has a slightly higher environmental impact than a control pavement.

The research on fiber-reinforced concrete (FRC) has demonstrated that dispersed metallic and non-metallic fibers help enhance the mechanical properties of concrete, especially tensile strength, tensile ductility, and resistance to crack opening and propagation (Brandt 2008). In recent years, as motivated by minimizing the environmental impact of the concrete industry, various types of fibers recycled from industrial wastes are added to concrete, e.g., steel fibers recovered from tires (Caggiano et al., 2017; Zhong et al. 2020), plastic fibers recycled from synthetic polymers (Merli et al. 2020), plant-based fibers recycled from agricultural and forest wastes (Wang et al. 2022; Ferreira et al. 2021). From the point of view of cutting carbon emissions, re-utilizing industrial wastes as an input of concrete extend the value of resources, which essentially contributes to the material efficiency strategy (U.S. Department of State and U.S. Executive Office of the President 2021). Caggiano et al. (2017) produced hybrid fibers reinforced concrete with recycled and industrial steel fibers (referred to as RSF and ISF, respectively). When used individually, as the average aspect ratio of RSF (around 110) was larger than that of ISF (around 60), the post-crack toughness of the concrete reinforced with the two fibers is almost comparable. When used together, the replacement of ISF with RSF will not substantially decay the post-cracking behavior of concrete, especially at a high replacement ratio. Zhong et al. (2020) produced concrete reinforced with recycled tire steel fibers (referred to as RTSF) of 0.5% to 0.9% by volume of concrete and virgin polypropylene fibers (referred to as PPF) of 0.1% to 0.5% by volume of concrete. Their test results show that the hybrid use of RTSF and PPF compensates for the workability loss caused by RTSF, and RTSF and PPF work synergistically together in enhancing the flexural toughness and crack resistance of concrete. Chen et al. (2021) developed a new sustainable fiber-reinforced rubberized cementitious composite (referred to as FRRC) using materials recycled from tires, including crumb rubber (CR) replacing 5% to 15% of the volume of fine aggregates, recycled tire steel fibers (RTSF) of 0.5% to 1.5% by volume of concrete, and recycled tire polymer fibers (RTPF) of 0.5% to 1.0% by volume of concrete. The FRRC has 41.6% lower drying shrinkage and 174% higher flexural strength than its cementitious composite matrix. More importantly, the FRRC has 13.3% to 68.2% lower production cost, embodied carbon, and embodied energy than its counterpart with industrial fibers, which suggests essential economic and environmental benefits. Regarding concrete reinforced with natural fibers derived from agricultural and forest wastes or industrial by-products, Wang et al. (2022) comprehensively reviewed the research from 2000 to 2021 on coir fibers and coir fiber reinforced cement-based composite materials. This review suggests that the coir fiber is an ideal substitution for other fibers (e.g., steel fiber, glass fiber, and carbon fiber) to produce FRCs, because of its low carbon footprint and large elongation in tension; However, some other plant-based fibers such as flax, sisal, hemp, and jute fibers are competitive than coir fibers with respect to the tensile strength and tensile modulus. In this context, Ferreira et al. (2021) studied the influence of environmental and internal relative humidity on the pullout behavior and tensile property of three types of natural fibers (i.e., curaua, jute, and sisal fibers). Their results show that the strengths of the fibers studied enhance at low levels of relative humidity, but drastically decrease at higher levels. Interestingly, Kilmartin-Lynch et al. (2021) explored the feasibility of using polypropylene fibers recycled from COVID-19 single-use face masks to improve the mechanical properties of concrete, and suggested that face masks are beneficial to the strength and overall quality of concrete especially when doses lower than 0.2% by volume of concrete. The above research has demonstrated the feasibility of FRCs with recycled fibers to enhance the sustainability of the concrete industry.

Attempts are also made on FRCs with micro fibers recycled from FRP waste. For instance, García et al. (2014) produced concrete with GFRP micro fibers recycled from four sources: streamlined fairings on trains, electrical panelboards, hulls for pleasure boats, and pultruded GFRP profiles. Their results show that the micro fibers significantly enhance both the compressive and flexural strengths of concrete even at a low fiber volume ratio. Baturkin et al. (2021) compared the influence of three forms of recycled FRP materials from decommissioned wind turbine blades, i.e., power, aggregate and micro fibers, on concrete performance, and suggested that recycling FRP waste into micro fibers is more beneficial to the mechanical properties than power and aggregate. Akbar and Liew (2020) investigated the influence of recycled carbon fibers (rCF) on the mechanical properties and environmental impacts of cement-based composites. Remarkable conclusions are made that the addition of 1% of rCF by volume of concrete leads to enhancements of 57%, 188% and 325% in elastic modulus, splitting tensile strength, and fracture toughness of concrete; resulting in 13.69% lower carbon emissions than plain cement paste; and saves 222% energy consumption and 70% economic cost than the counterpart with virgin carbon fibers. GFRP cylindrical needles with a diameter of 6 mm and a length of 100 mm cut from rebars, and GFRP prismatic needles with dimensions of 6 mm × 6 mm × 100 mm cut from decommissioned turbine blades were incorporated into concrete by Yazdanbakhsh et al. (2017, 2018) to partially replace the coarse aggregate in concrete. Their results showed that the flexural strength and toughness of concrete improved dramatically by using recycled GFRP needles. Zhou et al. (2021) used recycled GFRP fiber clusters and fibers as fibrous fillers in cement mortar, which resulted in enhanced mechanical properties and reduced shrinkage.

In a recent study, the authors of the present study proposed a mechanical method of recycling GFRP wind turbine blades into macro fibers, and demonstrated a concept of macro fiber-reinforced concrete (referred to as MFRC) (Fu et al. 2021). The results showed that the average splitting tensile strength and flexural strength of MFRC with a fiber volume ratio of 1.5% increased by 52% and 30%, respectively, as compared to those of plain concrete. However, the macro fibers used by Fu et al. (2021) were produced by cutting rough wind blade segments one-by-one into macro fibers with a fixed-length, e.g., 89.7 mm on average, therefore, the process of production is rather time-consuming and labor-intensive. As motivated by reducing production costs, the present study introduced a shredding machine to produce macro fibers with hybrid lengths of shorter than 100 mm. In comparison with the previous study (Fu et al. 2021), the macro fibers of hybrid lengths used herein will greatly reduce the manual work and energy consumption associated with cutting operations, and may also affect the mechanical properties due to the complexity of fiber geometry. To demonstrate the effect of changing macro fibers from a fixed-length to hybrid-lengths on the fresh and hardened properties of concrete, a series tests and a twice inverse analysis (Zhang et al. 2016) were performed.

2. EXPERIMENTAL PROGRAM

2.1 Recycling Waste Turbine Blades into Macro Fibers

The macro fibers used in the present study came from decommissioned turbine blades, as shown in Figure 1. The blades were cut up in the factory, and then screened for waste over 30 mm in length tentatively, which is referred to as the original GFRP waste here. A four-layer square-mesh sieve with the mesh sizes of 16 mm, 9.5 mm, 2.35 mm and 0 mm from top to bottom was used for sorting original GFRP waste. By artificially shaking the sieves, the waste retained on the top first and second layers was the target macro fibers, whereas the waste retained on the bottom sieve was the flakes and powder to be excluded. The operation process is detailed in Figure 2, after which about 30% by weight of the total waste was selected and re-used in concrete.

The above manual process, although perhaps the most efficient and least energy-consuming method of recycling macro fibers in the laboratory, may cause difficulties in (1) accurate determination of the physical parameters, e.g., length, width and thickness, of hybrid fibers; (2) thorough elimination of harmful ingredients that are mixed with fibers. When extending to industry, available machines can help reduce labor work and time as well as address the difficulties mentioned before with only slight energy consumption and carbon emissions. It is believed that the recycling method of the present study should be more competitive than other waste treatment methods, e.g., incineration or landfilling, with respect to economy and environmental impact. It should be noted that the retained waste powder and fine fibers can be re-utilized in concrete, which has been reported by many studies (Asokan 2010; Tittarelli 2013; Meira Castro et al. 2014) suggesting GFRP turbine blades are almost 100% recyclable.

2.2 Fiber Properties

The recycled macro fibers present highly variable lengths and widths, as shown in Figure 3. As such, geometric characterization was performed on a sample of 500 grams in weight. It should be noted the sample here was collected by weight rather than quantity [e.g., Fu et al. (2021) and Baturkin et al. (2021)], as the macro fibers used in the present study was characterized by hybrid lengths which is somewhat like concrete aggregate. The length, width and thickness of each fiber in the sample pool was measured with a digital caliper. The aspect ratio of each fiber was calculated by a ratio of length-to-width, following the definition of Fu et al. (2021).

Figure 4 shows the statistical characteristics of fiber dimensions. It is seen that the lengths were in the range of 27.9 mm to 81.6 mm with a mean value of 47.2 mm; the widths were in the range of 1.66 mm to 8.03 mm with a mean value of 3.64 mm; the thicknesses were in the range of 0.37 mm to 2.41 mm with a mean value of 0.97 mm; the aspect ratios were in the range of 4.02 to 32.5 with a mean value of 14.4. As expected, the dimensions of the recycled macro fibers used in the present study are rather dispersed as compared to those with almost fixed dimensions (Fu et al. 2021).

The tensile strength and tensile modulus of elasticity of the recycled macro fibers were 554.5 MPa, and 37.7 GPa, respectively, as determined following ASTM D3039/D3039M-08 (ASTM 2014). The average density of the fibers was 1820 kg/m^3 as per ASTM D792-20 (ASTM 2020).

2.3 Mix Design

The effect of doses of the recycled macro fibers on concrete performance was highlighted in the present study. Therefore, the dose of macro fibers expressed as a fraction of concrete volume (referred to as fiber volume fraction) was the only variable. Four groups of concrete with four fiber volume fractions were designed and tested, i.e., Groups CC, MFRC-0.5, MFRC-1.5 and MFRC-2.5 for fiber volume fractions of 0%, 0.5%, 1.5% and 2.5%, respectively. The group name CC indicates the control concrete (plain concrete without fiber reinforcement); each name of the other three groups consists of a term MFRC which is short for macro fiber reinforced concrete, and a decimal indicating the fiber volume fraction in percentage.

Table 1 shows the mix proportions for all groups. The mixes all had the same proportions of cement, water, fine aggregate, coarse aggregate and superplasticizer which were the control group; the main difference between the mixes was the fiber volume fraction. The control group (i.e., the concrete matrix of all MFRCs) was designed with a compressive strength of 40 MPa and a slump of 185 mm. The binder material was a P.O. 42.5 ordinary Portland cement (OPC) without the addition of any supplemental cementitious material. Local tap water in Guangzhou, China, was used as the mixing water. The fine aggregate was natural river sand with a maximum particle size of 5 mm and a fineness modulus of 2.45. The coarse aggregate was granite gravel with the particle size ranging from 5 mm to 20 mm. A polycarboxylate superplasticizer with a water reducing efficiency of 20% was added 0.25% by weight of cement to compensate for the workability loss caused by the incorporation of macro fibers.

2.4 Specimen Preparation

Four batches of concrete corresponding to the four groups of the present study were cast following a procedure developed by Fu et al. (2021). First, cement, fine aggregate and coarse aggregate were mixed for 1 minute; Second, superplasticizer and water were added slowly and kept mixing for 2 minutes; Third, the macro fibers were added in a similar way and kept mixing until it is evenly distributed in the concrete; Fourth, casting. The specimens were demolded at 24 hours after concrete casting, immediately sealed with plastic films, and stored in the ambient environment for 28 days. Spraying water was performed every day to maintain a high humidity during concrete curing.

2.5 Test Methods

The workability of each group was evaluated by testing the slump of fresh concrete in accordance with ASTM C143 (ASTM 2020). The slump value was averaged from three readings and approximated to the nearest 5 mm.

The compressive strength of each group was determined by three concrete cylinders with a diameter of 150 mm and a height of 300 mm following ASTM C39 (ASTM 2021). The modulus of elasticity and Poisson's ratio were determined by the same cylinders following ASTM C469 (ASTM 2014).

The flexural performance of each group was evaluated by four-point bending tests on three short beams with dimensions of 150 mm × 150 mm × 550 mm. The beam tests were carried out using an electro-hydraulic servo test machine following ASTM C1609 (ASTM 2012). As detailed in Figure 5, a rubber sheet was placed between the actuator and the specimen to distribute the compressive load; a pair of LVDTs were mounted on a precisely machined test jig which was clamped to the specimen, to measure the net mid-span deflection; the supports ensured in-plane and out-plane rotation of the beam, as well as the sliding along the longitudinal direction. The bending tests were performed with a loading rate of 0.05 mm/min and terminated when the net deflection reached 3.5 mm. Afterward, the whole load-displacement curve of each specimen, the peak load (P_p), the deflection at peak load (δ_p), the residual loads, P_{600} and P_{150}, at net deffections of $L/600$ (i.e., 450 mm/600 = 0.75 mm) and $L/150$ (i.e., 450 mm/150 = 3 mm), respectively, were recorded. The peak strength (f_p), the residual strengths, f_{600} and f_{150}, were calculated according to the following equation (ASTM 2019):

$$f = \frac{PL}{bd^2} \tag{1}$$

where P is the load; L is the beam span; b and d are the width and depth of the beam. Toughness (T_{150}) is defined as the area under the load-displacement curve with deflection from 0 to $L/150$.

3. RESULTS AND DISUCCSION

3.1 Workability of Fresh Concrete

The average slumps of Groups CC, MFRC-0.5, MFRC-1.5 and MFRC-2.5 were 190 mm, 153 mm, 122 mm and 87 mm, respectively. It is shown that the workability of concrete decreased with increasing fiber volume ratio. Although with the help of superplasticizer, all groups achieved a slump of larger than 80 mm which meets the requirement of filed applications (Patel et al. 2019; Nematollahi et al. 2014), the negative effect of macro fibers on the workability is rather obvious as indicated by a 54% of slump loss resulted from the adding of 2.5% of macro fibers. The same phenomenon was observed in other researches (Paktiawal et al. 2021; Teja Prathipati et al. 2021). As the proportion of fibers increases, the surface area of the fibers that needed to be covered by the water film also increased, thereby reducing the free water in the concrete. Moreover, the morphology of the fiber used in this study was irregular due to the randomness of the shredding. This resulted in an increase in the surface area of the fiber, meaning that the reduction effect is more pronounced compared to morphologically intact fibers. It should be noted that during concrete casting, no segregation of fibers was observed, suggesting that the recycled macro fibers have a relatively good bond to fresh concrete due to its rough surface that naturally formed during mechanical crashing and cutting.

3.2 Compressive Behavior

Figure 6 shows the failure patterns of all groups. It is seen that the specimens in the control group (see Figure 6a) and those with a fiber volume ratio being as low as 0.5% (see Figure 6b) to showed a conical or conical-shear type of fracture, which were both typical failure patterns for concrete without or just with a slight reinforcement per ASTM C39/C39M (ASTM 2021). The only exception was the middle specimen in Figure 6b showing a shear type fractural pattern, which may be understood by the scatter of fiber distribution at a low volume ratio, e.g., 0.5%. By contrast, the specimens with higher fiber volume ratios (see Figure 6c and 6d) retained their integrity with much less concrete spalling but more cracks, which was different from those specified in ASTM C39/C39M (ASTM 2021). Spalling appeared at the top region of Specimen MFRC-1.5-1 (Left of Figure 5c) while at the bottom part for Specimen MFRC-1.5-3 (Middle of Figure 5c). Such a phenomenon might be attributed to the fact that macro fibers are more difficult than micro fibers to be evenly distributed in a cylinder specimen to provide sufficient reinforcement to all regions. The added macro fibers changed the failure pattern of concrete as the fibers bridged concrete cracks and impeded crack propagation, thereby leading to a more ductile failure pattern (Wang et al. 2019; Khan et al. 2020).

Figure 7 shows the compressive stress-strain curves of all groups. The ascending branch of the curves shows to be close to each other, implying that the added macro fibers had not been mobilized at this stage. After the compressive stress of concrete reaches about 80% the peak stress, the cracks in concrete became more significant. At this stage, the macro fibers incorporated in concrete become mobilized, and constrain the development of the cracks. The descending branch of the stress-strain curve therefore became more gradual with an enhanced toughness due to the increase of fiber volume ratio. Such observations confirm a ductile failure process of concrete with macro fibers. Another major effect resulting from the incorporation of the macro fibers is the slight decrease in the peak value of the curves as illustrated in details in the following paragraph.

Table 2 shows the key results of compression tests. It is seen that the adding of macro fibers of 0.5%, 1.5% and 2.5% by volume decreased the peak compressive stress (i.e., compressive strength) by 3.95%, 6.81% and 14.07%, respectively, as compared to the control group. Besides, the concrete reinforced with macro fibers showed a Poisson's ratio in the range of 0.14 to 0.15, which is 16.7% higher than 0.12, i.e., a typical value of the conventional concrete. With respect to the modulus of elasticity, 0.5% of macro fibers resulted in an improvement of 12.4% than that of the control group, however, on the contrary, further increase of fiber volume ratio led to decreases in the modulus of elasticity.

The above test results indicate that the incorporation of macro fibers negatively affects the compressive strength of concrete, but enhances the toughness under compression. Similar observations were also made on concrete reinforced with short fibers (Dehghan et al. 2017) and macro fibers (Fu et al. 2021). The detrimental effect of macro fibers on compressive strength could be understood that the rough but loose surface of a macro fiber that formed during mechanical recycling results in a weak bond to concrete matrix, and the mechanism will be highlighted when harmful ingredients that cannot be eliminated in manual sieving are mixed with fibers (Yao et al. 2003; Ranjbar et al. 2020). In addition, the positive effect of macro fibers on toughness and Poisson's ratio could be explained by the bridging of macro fibers to cracks in concrete, which leads to larger axial deformation and dilation under compression.

3.3 Flexural Behavior

Figure 8 shows the failure patterns of all groups after flexural tests. The specimens in the control groups crushed suddenly after the initiation of micro cracks, whereas the specimens reinforced with macro fibers continued to sustain flexural loading in company with crack propagation for a long period. The distinct failure pattern of the latter is attributed to the bridging effect of macro fibers on concrete cracking, which contributes to the residual capacity to resist flexural loading after crack initiation. The concrete crack propagates intersecting a number of macro fibers distributed in concrete, and the further development of the crack has been therefore mitigated by these bridging macro fibers.

Figure 10 shows the flexural load-deflection curves of all groups, in which Figure 10(a) gives the complete curves with deflection up to 3.5 mm, and Figure 10(b) gives the initial portions with deflection up to 1.0 mm. Similar to the flexural load-deflection behaviors of the concrete reinforced by various amounts of macro fibers with a fixed-length, Group MFRC-0.5 that incorporated a slight amount of macro fibers showed a typical deflection softening curve (Naaman 2003), and Groups MFRC-1.5 and MFRC-2.5 showed a typical deflection hardening curve (Naaman 2003), as depicted in Figure 11. For the former, as its fiber volume ratio was low, the majority of macro fibers broke or pulled-out once the load reached the peak value, therefore the load gradually decreased with the increasing deflection after the peak point that represented the first cracking. However, for the latter two groups, after the first cracking of concrete matrix, the cross-sectional tensile stress redistributed and transferred to the macro fibers across cracks. As their fiber volume ratios were relatively high, the macro fibers can help the beam resist a higher flexural loading, thus led to a continuous increase in the load with increasing deflection and also caused a change of flexural stiffness. Besides, it is interesting to note that deflection hardening branch was prolonged with increasing fiber volume ratio, but the stiffness of this branch was seen not dependent on the amount of macro fibers.

The key results of flexural tests are given in Table 3. The flexural strength increased from 3.91 MPa of the control group to 4.08 MPa (4.34% of improvement), 4.43 MPa (13.30% of improvement) and 5.39 MPa (37.85% of improvement), respectively, for the groups with fiber volume ratios of 0.5%, 1.5% and 2.5%. Move obviously, the flexural toughness for the groups with fiber volume ratios of 0.5%, 1.5% and 2.5% improved by 15.5, 22.7, and 36.8 times as compared to the control group. The improved flexural toughness was caused by the increased residual strength of concrete at the post-peak deflection softening branch of the flexural load-deflection curve, e.g., the residual strength at a deflection of L/600 (f_{600}) increased from zero of the control group to 1.63 MPa, 1.96 MPa and 3.84 MPa, for the groups with fiber volume ratios of 0.5%, 1.5% and 2.5%, respectively. The test results show that, similar to the findings on macro fibers with fixed lengths (Fu et al. 2021), the incorporation of macro fibers with hybrid lengths can also improve the flexural strength and toughness of concrete beams. Moreover, the improvement become more obvious with increasing fiber volume ratio.

3.4 Inverse Analysis Based on the Results of Four-Point Bending

The tensile stress-strain (σ-ε) behavior of concrete that required by structural analysis is normally based on direct-tensile test results. However, to the best of the authors' acknowledgement, there is currently no standardized method for direct-tensile tests on fiber-reinforced concrete, especially for the concrete reinforced by macro fibers. The difficulties may include: (1) reasonable determination of the specimen's dimensions considering the length and alignment of fibers; (2) prevention of eccentric stressing; and (3) minimization of the effect of clamping on the tensile test results (Barragán et al. 2003; Hassan et al. 2012; Tran et al. 2014; Wille et al. 2014). To eliminate the complexity associated with direct-tensile tests, the present study utilized a twice inverse analysis method (TIAM) to predict the uniaxial tensile stress-strain behavior of concrete with the load-deflection curves given by four-point bending tests.

There currently has many TIAMs aiming at determination of the constitutive laws of concrete, e.g., the TIAM utilized in Ferreira et al., (2016) is to predict the bond-slip law of jute fibers embedded in a cementitious matrix; by contrast, the TIAM developed by López (2014) is to predict the uniaxial tensile stress-strain law of ultra-high-performance fiber-reinforced concrete (UHPFRC). The latter is adopted in the present study to predict the uniaxial tensile stress-strain behavior of the concrete reinforced with recycled macro fibers. The TIAM of López (2014) is based on two transformations: first, δ to ϕ transformation, which transforms the mid-span deflection (δ) of a beam to the bending curvature (ϕ) of the mid-span cross-section of the beam in accordance with Timoshenko beam theory; and second, M-ϕ to σ-ε transformation, which transforms the bending moment-curvature (M-ϕ) behavior of the mid-span cross-section of the beam to the uniaxial tensile stress-strain (σ-ε) behavior of concrete. It should be noted that the tensile stress-strain (σ-ε) behavior predicted by TIAM is slightly different from that given by real direct-tensile tests (Zhang et al. 2016). However, due to the aforementioned difficulties of direct-tensile tests, it is hard to say which is right or wrong. At least the logic and mathematics of TIAM are strict and consistent with the principles of structural analysis, therefore it is used by the authors in the present study.

The TIAM was implemented in a MATLAB program. The specimens in the control group were excluded from the inverse analysis, as their flexural load-deflection curves lack of post-peak portions. Besides, 150 to 200 points on the flexural load-deflection curve of each specimen were selected to perform the inverse analysis to improve the accuracy of analysis.

The predicted direct-tensile stress-strain curves are given in Figure 12. It should be noted that the curves in Figure 12 are smoothed for ease of comparison. It is not supervising that the curves generally reflect the effect of macro fibers on the tensile behavior of concrete, i.e., enhances the tensile strength and toughness of concrete. The direct-tensile strengths and strain predicted by the inverse analysis are collected in Table 4. It is seen that the tensile strength increases from 2.05 to 2.26 MPa, with the corresponding tensile strain increases from 77.3 to 134.0 με, as the fiber volume ratio increases from 0.5% to 2.5%. The predictions suggest that the tensile strength and toughness increase with increasing fiber volume ratio.

4. APPLICATION POTENTIAL

The macro fibers have dimensions and mechanical properties similar to those of steel fibers, and thus play similar roles in constraining crack propagation and enhancing the tensile properties of concrete. Therefore, the macro fibers recycled from waste FRP composites could be able to replace the pricey steel fibers incorporated into concrete for a number of field applications (e.g., highway lining, tunnel lining, and runway).

5. CONCLUSIONS

The present study has been focused on concrete incorporating macro fibers with hybrid lengths recycled from waste GFRP wind turbine blades (MFRC). Experiments and an inverse analysis were carried out to characterize the effect of fiber volume ratio on the mechanical properties of concrete. The following conclusions can be drawn based on the results and discussion:

1. The incorporation of recycled macro fibers with hybrid lengths resulted in a larger surface area around which the formation of water film requires more free water, thus decreasing the slump from 190 mm to 87 mm as the fiber volume ratio increased from 0 to 2.5%.

2. The combination of the two mechanisms introduced by the incorporation of macro fibers resulted in less concrete spalling at specimen failure, and a more gradual descending branch of the stress-strain curves, but a reduction in the compressive strength up to 14.1% at a fiber volume ratio of 2.5%.

3. The incorporated macro fibers effectively constrained the development of concrete cracks, thus enhancing both the flexural strength and toughness of MFRC, which at the fiber volume ratio of 2.5% are respectively 37.9% and 36.8 times higher than those of the control concrete without macro fibers.

4. A twice inverse analysis was performed to efficiently convert the direct-tensile stress-strain curve of MFRC from the load-deflection results of beam specimens, confirming the beneficial effect of macro fibers on the tensile behavior of concrete. The tensile strength of MFRC predicted using TIAM increased from 2.05 MPa to 2.26 MPa, when the fiber volume ration increased from 0.5% to 2.5%.

Based on the experimental observations, it is believed that the macro fibers with hybrid lengths made from decommissioned turbine blades can significantly enhance the flexural properties, tensile properties and toughness of concrete, but it has a negative effect on compression behavior. Compared with the macro fibers with a fixed-length, the production process of the fibers with hybrid lengths is less time-consuming and labor-intensive, and is more suitable for industrialization. This study provides a feasible and economical path for the recovery of GFRP waste.

CREDIT AUTHORSHIP CONTRIBUTION STATEMENT

Guang-Ti Xu: Methodology, Investigation, Formal analysis, Visualization, Writing - original draft. **Ming-Jie Liu**: Methodology, Investigation. **Yu Xiang**: Methodology, Visualization, Writing - review & editing. **Bing Fu**: Conceptualization, Methodology, Supervision, Visualization, Writing - review & editing, Project administration, Funding acquisition.

DECLARATION OF COMPETING INTEREST

The authors declare that they have no known competing financial interests or personal relationships that could have appeared to influence the work reported in this paper.

ACKNOWLEDGEMENTS

The authors gratefully acknowledge the financial support provided by the National Natural Science Foundation of China (Project Nos: 52178212 and 51978176), the Hong Kong Research Grants Council (Project No: T22-502/18-R) and National Innovation and Entrepreneurship Training Program for Undergraduate (Project No: 202110559051).

REFERENCES

ASTM. (2014). *Standard test method for tensile properties of polymer matrix composite materials*. D3039/D3029M-08, West Conshohocken, PA: ASTM.

ASTM. (2014). *Standard Test Method for Static Modulus of Elasticity and Poisson's Ratio of Concrete in Compression*. ASTM C469/C469M-14, West Conshohocken, PA: ASTM.

ASTM. (2021). *Standard Test Method for Compressive Strength of Cylindrical Concrete Specimens*. ASTM C39/C39M-21, West Conshohocken, PA: ASTM.

ASTM. (2020). *Standard Test Method for Slump of Hydraulic-Cement Concrete*. ASTM C143/C143M-15a, West Conshohocken, PA: ASTM.

ASTM. (2019). *Standard Test Method for Flexural Performance of Fiber-Reinforced Concrete (Using Beam with Third-Point Loading)*. ASTM C1609/C1609M-19, West Conshohocken, PA: ASTM.

ASTM. (2020). *Standard Test Methods for Density and Specific Gravity (Relative Density) of Plastics by Displacement*. ASTM D792-20, West Conshohocken, PA: ASTM.

Akbar, A., & Liew, K. M. (2020). Assessing recycling potential of carbon fiber reinforced plastic waste in production of eco-efficient cement-based materials. *Journal of Cleaner Production*, *274*.

Asokan, P., Osmani, M. & Price, A. D. F. (2009). Assessing the recycling potential of glass fibre reinforced plastic waste in concrete and cement composites. *Journal of Cleaner Production,* 17, 821-829.

Asokan, P., Osmani, M. & Price, A. D. F. (2010). Improvement of the mechanical properties of glass fiber reinforced plastic waste powder filled concrete. *Construction and Building Materials*, 24, 448-460.

Barragán, B. E., Gettu, R., Martín, M. A. & Zerbino, R. L. (2003). Uniaxial tension test for steel fibre reinforced concrete—a parametric study. *Cement and Concrete Composites,* 25, 767-777.

Baturkin, D., Hisseine, O. A., Masmoudi, R., Tagnit-Hamou, A. & Massicotte, L. (2021). Valorization of recycled FRP materials from wind turbine blades in concrete. *Resources, Conservation and Recycling,* 174.

Bouckaert, S., Fernandez Pales, A., McGlade, C., Remme, U., Wanner, B., Varro, L., D'Ambrosio, D., & Spencer, T. (2021). *Net Zero by 2050: A Roadmap for the Global Energy Sector*. International Energy Agency, Paris, France, 1-224.

Brandt, A. M. (2008). Fibre reinforced cement-based (FRC) composites after over 40 years of development in building and civil engineering. *Composite Structures*, *86*(1-3), 3-9.

Caggiano, A., Folino, P., Lima, C., Martinelli, E., & Pepe, M. (2017). On the mechanical response of hybrid fiber reinforced concrete with recycled and industrial steel fibers. *Construction and Building Materials*, *147*, 286-295.

Chen, M., Zhong, H., Chen, L., Zhang, Y., & Zhang, M. (2021). Engineering properties and sustainability assessment of recycled fibre reinforced rubberised cementitious composite. *Journal of Cleaner Production*, *278*.

Colombo, B., Gaiardelli, P., Dotti, S. & Caretto, F. (2022). Recycling technologies for fibre-reinforced plastic composite materials: A bibliometric analysis using a systematic approach. *Journal of Composite Materials*, 00219983221109877.

Correia, J. R., Almeida, N. M. & Figueira, J. R. (2011). Recycling of FRP composites: reusing fine GFRP waste in concrete mixtures. *Journal of Cleaner Production,* 19, 1745-1753.

Dehghan, A., Peterson, K. & Shvarzman, A. (2017). Recycled glass fiber reinforced polymer additions to Portland cement concrete. *Construction and Building Materials*, 146, 238-250.

Ferreira, S. R., Martinelli, E., Pepe, M., De Andrade Silva, F., & Toledo Filho, R. D. (2016). Inverse identification of the bond behavior for jute fibers in cementitious matrix. *Composites Part B: Engineering*, 95, 440-452.

Ferreira, S. R., Mendes de Andrade, R. G., Koenders, E., de Andrade Silva, F., de Moraes Rego Fairbairn, E., & Toledo Filho, R. D. (2021). Pull-out behavior and tensile response of natural fibers under different relative humidity levels. *Construction and Building Materials*, *308*.

Fu, B., Liu, K. C., Chen, J. F. & Teng, J. G. (2021). Concrete reinforced with macro fibres recycled from waste GFRP. *Construction and Building Materials,* 310, 125063.

García, D., Vegas, I. & Cacho, I. (2014). Mechanical recycling of GFRP waste as short-fiber reinforcements in microconcrete. *Construction and Building Materials,* 64, 293-300.

Goncalves, R. M., Martinho, A. & Oliveira, J. P. (2022). Recycling of Reinforced Glass Fibers Waste: Current Status. *Materials (Basel)*, 15.

GWEC. (2022). *Global Wind Report 2022*, Global Wind Energy Council, Brussels, Belgium, 1-154.

Hassan, A. M. T., Jones, S. W. & Mahmud, G. H. (2012). Experimental test methods to determine the uniaxial tensile and compressive behaviour of ultra high performance fibre reinforced concrete (UHPFRC). *Construction and Building Materials,* 37, 874-882.

Hollaway, L. C. (2010). A review of the present and future utilisation of FRP composites in the civil infrastructure with reference to their important in-service properties. *Construction and Building Materials,* 24, 2419-2445.

Hong Kong Special Administrative Region. (2021). *Hong Kong's Climate Action Plan 2050*.

IEA. (2021). *Wind Power*. International Energy Agency, Paris, France.

IPCC. (2021). Summary for Policymakers. In: Climate Change 2021: The Physical Science Basis. Contribution of Working Group I to the Sixth Assessment Report of the Intergovernmental

Panel on Climate Change [Masson-Delmotte, V., P. Zhai, A. Pirani, S.L. Connors, C. Péan, S. Berger, N. Caud, Y. Chen, L. Goldfarb, M.I. Gomis, M. Huang, K. Leitzell, E. Lonnoy, J.B.R. Matthews, T.K. Maycock, T. Waterfield, O. Yelekçi, R. Yu, and B. Zhou (eds.)]. Cambridge University Press, Cambridge, United Kingdom and New York, NY, USA, In press, doi:10.1017/9781009157896.

Jacob, A. (2011). Composites can be recycled. *Reinforced Plastics,* 55, 45-46.

Jensen, J. P., & Skelton, K. (2018). Wind turbine blade recycling: Experiences, challenges and possibilities in a circular economy. *Renewable and Sustainable Energy Reviews*, *97*, 165-176.

Job, S. (2013). Recycling glass fibre reinforced composites – history and progress. *Reinforced Plastics,* 57, 19-23.

Khan, M., Cao, M. & Ali, M. (2020). Cracking behaviour and constitutive modelling of hybrid fiber reinforced concrete. *Journal of Building Engineering*, 30, 101272.

Kilmartin-Lynch, S., Saberian, M., Li, J., Roychand, R., & Zhang, G. (2021). Preliminary evaluation of the feasibility of using polypropylene fibres from COVID-19 single-use face masks to improve the mechanical properties of concrete. *Journal of Cleaner Production*, *296*, 126460.

Liu, P., & Barlow, C. Y. (2017). Wind turbine blade waste in 2050. *Waste Management*, *62*, 229-240.

López, J. Á., Serna, P., Navarro-Gregori, J. & Camacho, E. (2014). An inverse analysis method based on deflection to curvature transformation to determine the tensile properties of UHPFRC. *Materials and Structures,* 48, 3703-3718.

Meira Castro, A. C., Carvalho, J. P., Ribeiro, M. C. S., Meixedo, J. P., Silva, F. J. G., Fiúza, A. & Dinis, M. L. (2014). An integrated recycling approach for GFRP pultrusion wastes: recycling and reuse assessment into new composite materials using Fuzzy Boolean Nets. *Journal of Cleaner Production*, 66, 420-430.

Merli, R., Preziosi, M., Acampora, A., Lucchetti, M. C., & Petrucci, E. (2020). Recycled fibers in reinforced concrete: A systematic literature review. *Journal of Cleaner Production*, *248*.

Naaman, A. E. (2003). Engineered Steel Fibers with Optimal Properties for Reinforcement of Cement Composites. *Journal of Advanced Concrete Technology*, 1 (3): 241-252.

Nagle, A. J., Delaney, E. L., Bank, L. C., & Leahy, P. G. (2020). A Comparative Life Cycle Assessment between landfilling and Co-Processing of waste from decommissioned Irish wind turbine blades. *Journal of Cleaner Production*, *277*.

Nematollahi, B. & Sanjayan, J. (2014). Properties of Fresh and Hardened Glass Fiber Reinforced Fly Ash Based Geopolymer Concrete. *Key engineering materials*, 594-595.

Oliveux, G., Dandy, L. O. & Leeke, G. A. (2015). Current status of recycling of fibre reinforced polymers: Review of technologies, reuse and resulting properties. *Progress in Materials Science,* 72, 61-99.

Paktiawal, A. & Alam, M. (2021). Alkali-resistant glass fiber high strength concrete and its durability parameters. *Materials Today: Proceedings*, 47, 4758-4766.

Passarelli, D., Denton, F., & Day, A. (2021). Beyond Opportunism: The UN Development System's Response to the Triple Planetary Crisis. United Nations University, New York, the United States, 1-21.

Patel, K., Gupta, R., Garg, M., Wang, B. & Dave, U. (2019). Development of FRC Materials with Recycled Glass Fibers Recovered from Industrial GFRP-Acrylic Waste. *Advances in Materials Science and Engineering*, 2019, 1-15.

Pickering, S. J. (2006). Recycling technologies for thermoset composite materials—current status. *Composites Part A: Applied Science and Manufacturing,* 37, 1206-1215.

Pierrehumbert, R. (2019). There is no Plan B for dealing with the climate crisis. Bulletin of the Atomic Scientists, 75(5), 215-221.

Ranjbar, N., Talebian, S., Mehrali, M., Kuenzel, C., Cornelis Metselaar, H. S. & Jumaat, M. Z. (2016). Mechanisms of interfacial bond in steel and polypropylene fiber reinforced geopolymer composites. *Composites Science and Technology,* 122, 73-81.

Ranjbar, N. & Zhang, M. (2020). Fiber-reinforced geopolymer composites: A review. *Cement and Concrete Composites,* 107, 103498.

Ribeiro, M. C. S., Meira-Castro, A. C., Silva, F. G., Santos, J., Meixedo, J. P., Fiúza, A., Dinis, M. L. & Alvim, M. R. (2015). Re-use assessment of thermoset composite wastes as aggregate and filler replacement for concrete-polymer composite materials: A case study regarding GFRP pultrusion wastes. *Resources, Conservation and Recycling,* 104, 417-426.

Scaffaro, R., Di Bartolo, A. & Dintcheva, N. T. (2021). Matrix and Filler Recycling of Carbon and Glass Fiber-Reinforced Polymer Composites: A Review. *Polymers (Basel),* 13.

Shahria Alam, M., Slater, E. & Muntasir Billah, A. (2013). Green concrete made with RCA and FRP scrap aggregate: fresh and hardened properties. *Journal of materials in civil engineering,* 25, 1783-1794.

Singh, A., Charak, A., Biligiri, K. P., & Pandurangan, V. (2022). Glass and carbon fiber reinforced polymer composite wastes in pervious concrete: Material characterization and lifecycle assessment. *Resources, Conservation and Recycling*, *182*.

Tittarelli, F. & Moriconi, G. (2010). Use of GRP industrial by-products in cement based composites. *Cement and Concrete Composites,* 32, 219-225.

Tittarelli, F. (2013). Effect of low dosages of waste GRP dust on fresh and hardened properties of mortars: Part 2. *Construction and Building Materials*, 47, 1539-1543.

Tran, T. K., Kim, D. J. & Choi, E. (2014). Behavior of double-edge-notched specimens made of high performance fiber reinforced cementitious composites subject to direct tensile loading with high strain rates. *Cement and Concrete Research,* 63, 54-66.

U.K. Department for Business, Energy & Industrial Strategy. (2021). *Net Zero Strategy: Build Back Greener*. London, the United Kingdom, 1-368.

United Nations. (2015). *Paris Agreement*. Paris, France, 1-25.

U.S. Department of State and U.S. Executive Office of the President. (2021). *The Long-Term Strategy of the United States: Pathways to Net-Zero Greenhouse Gas Emissions by 2050*. Washington, D.C., the United States, 1-61.

Wang, B., Yan, L. B., & Kasal, B. (2022). A review of coir fibre and coir fibre reinforced cement-based composite materials (2000–2021). *Journal of Cleaner Production*, *338*.

Wang, D., Ju, Y., Shen, H. & Xu, L. (2019). Mechanical properties of high performance concrete reinforced with basalt fiber and polypropylene fiber. *Construction and Building Materials*, 197, 464-473.

Wille, K., El-Tawil, S. & Naaman, A. E. (2014). Properties of strain hardening ultra high performance fiber reinforced concrete (UHP-FRC) under direct tensile loading. *Cement and Concrete Composites,* 48, 53-66.

Witten, E. (2020). The market for glass fibre reinforced plastics (GRP) in 2020. *Market Developments, Trends, Outlooks and Challenges. Federation of Reinforced Plastics*.

Yang, Y., Boom, R., Irion, B., van Heerden, D.-J., Kuiper, P. & de Wit, H. (2012). Recycling of composite materials. *Chemical Engineering and Processing: Process Intensification,* 51, 53-68.
Yao, W., Li, J. & Wu, K. (2003). Mechanical properties of hybrid fiber-reinforced concrete at low fiber volume fraction. *Cement and concrete research,* 33, 27-30.
Yazdanbakhsh, A. & Bank, L. (2014). A Critical Review of Research on Reuse of Mechanically Recycled FRP Production and End-of-Life Waste for Construction. *Polymers*, 6, 1810-1826.
Yazdanbakhsh, A., C. Bank, L. & Chen, C. (2016). Use of recycled FRP reinforcing bar in concrete as coarse aggregate and its impact on the mechanical properties of concrete. *Construction and Building Materials,* 121, 278-284.
Yazdanbakhsh, A., Bank, L. C., Chen, C., and Tian, Y. (2017). FRP-needles as discrete reinforcement in concrete. *Journal of Materials in Civil Engineering*, 29 (10): 04017175.
Yazdanbakhsh, A., Bank, L. C., Rieder, K.-A., Tian, Y. & Chen, C. (2018). Concrete with discrete slender elements from mechanically recycled wind turbine blades. *Resources, Conservation and Recycling,* 128, 11-21.
Zhang, Z., Shao, X., Zhu, P. & Li, W. (2016). Twice inverse analysis method based on four-point bending test results for UHPC tensile behavior characterization. *China Civil Engineering Journal,* 49, 77-86. (in Chinese)
Zhong, H., & Zhang, M. (2020). Experimental study on engineering properties of concrete reinforced with hybrid recycled tyre steel and polypropylene fibres. *Journal of Cleaner Production*, *259*.
Zhou, B., Zhang, M., Wang, L. & Ma, G. (2021). Experimental study on mechanical property and microstructure of cement mortar reinforced with elaborately recycled GFRP fiber. *Cement and Concrete Composites,* 117, 103908.

Tables

Table 1. Concrete mix proportions (Unit: kg/m³).

Group	Cement	Water	Sand	Granite Gravel	Superplasticizer	Macro Fiber
CC	395	189.6	727	1137	0.98	0
MFRC-0.5	395	189.6	727	1137	0.98	9.1
MFRC-1.5	395	189.6	727	1137	0.98	27.3
MFRC-2.5	395	189.6	727	1137	0.98	45.5

Table 2. Key results of compression tests.

Specimen	f_c (MPa)	ε_{co} (%)	E (GPa)	v
CC-1	33.91	0.261	19.47	0.13
CC-2	33.80	0.239	20.05	0.11
CC-3	33.81	0.253	17.47	0.11
Mean	33.84	0.251	18.99	0.12
Standard deviation	0.06	0.01	1.35	0.01
MFRC0.5-1	32.34	0.238	21.17	0.14
MFRC0.5-2	32.98	0.256	21.81	0.12
MFRC0.5-3	32.33	0.233	21.08	0.17
Mean	32.55	0.246	21.35	0.14
Standard deviation	0.37	0.01	0.40	0.03
MFRC1.5-1	31.04	0.268	19.03	0.13
MFRC1.5-2	31.82	0.278	22.01	0.17
MFRC1.5-3	31.87	0.306	18.67	0.12
Mean	31.58	0.284	19.90	0.14
Standard deviation	0.46	0.02	1.83	0.03
MFRC2.5-1	29.28	0.237	18.12	0.16
MFRC2.5-2	28.76	0.229	19.16	0.16
MFRC2.5-3	29.33	0.253	18.74	0.14
Mean	29.12	0.239	18.67	0.15
Standard deviation	0.31	0.01	0.52	0.01

Note: f_c is peak compressive stress; ε_o is the strain at peak compressive stress; E is modulus of elasticity; v is Poisson's ratio.

Table 3. Key results of flexural tests.

No.	P_p (kN)	f_p (MPa)	δ_p (mm)	P_{600} (kN)	P_{150} (kN)	f_{600} (MPa)	f_{150} (MPa)	T_{150} (J)
CC-1	25.98	4.23	0.073	0.0	0.0	0.0	0.0	1.97
CC-2	22.83	3.72	0.082	0.0	0.0	0.0	0.0	1.29
CC-3	23.21	3.78	0.078	0.0	0.0	0.0	0.0	1.30
Mean	24.01	3.91	0.078	0.0	0.0	0.0	0.0	1.52
Standard deviation	1.72	0.28	0.005	0.0	0.0	0.0	0.0	0.39
MFRC0.5-1	23.69	3.86	0.062	9.34	3.15	1.52	0.51	23.38
MFRC0.5-2	26.22	4.27	0.098	10.31	2.77	1.68	0.45	25.19
MFRC0.5-3	25.31	4.12	0.089	10.35	3.52	1.69	0.57	26.16
Mean	25.07	4.08	0.083	10.00	3.15	1.63	0.51	24.91
Standard deviation	1.28	0.21	0.019	0.57	0.38	0.10	0.06	1.41
MFRC1.5-1	25.61	4.17	0.127	13.76	7.24	2.24	1.18	40.10
MFRC1.5-2	26.55	4.33	0.209	12.04	4.12	1.96	0.67	32.18
MFRC1.5-3	29.32	4.78	0.157	10.39	6.88	1.69	0.81	35.61
Mean	27.16	4.43	0.164	12.06	6.08	1.96	0.89	35.96
Standard deviation	1.93	0.32	0.041	1.69	1.71	0.28	0.26	3.97
MFRC2.5-1	35.99	5.87	0.248	26.13	8.77	4.26	1.41	60.72
MFRC2.5-2	31.16	5.08	0.329	23.09	10.46	3.76	1.70	57.87
MFRC2.5-3	32.09	5.23	0.285	24.52	8.66	3.51	1.41	53.67
Mean	33.08	5.39	0.287	24.58	9.30	3.84	1.51	57.42
Standard deviation	2.56	0.42	0.041	1.52	1.01	0.38	0.17	3.55

Table 4. Key results of inverse analyses.

No.	Tensile strength f_t (MPa)	Tensile strain ε_t (με)
MFRC0.5-1	2.05	58.3
MFRC0.5-2	2.05	76.3
MFRC0.5-3	2.04	97.2
Mean	2.05	77.3
Standard deviation	0.01	19.5
MFRC1.5-1	2.12	136.9
MFRC1.5-2	2.33	83.1
MFRC1.5-3	2.17	108.1
Mean	2.21	109.4
Standard deviation	0.11	29.9
MFRC2.5-1	2.37	117.0
MFRC2.5-2	2.24	188.3
MFRC2.5-3	2.17	96.6
Mean	2.26	134.0
Standard deviation	0.10	48.15

Figures

Figure 1. Decommissioned wind turbine blades.

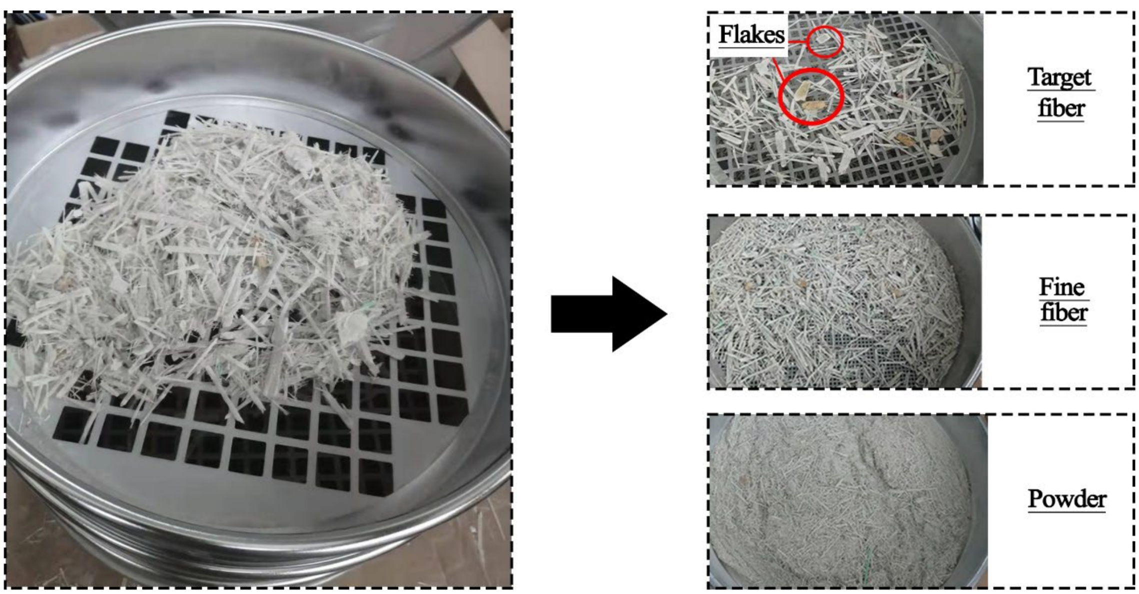

Figure 2. Process of selecting macro fibers.

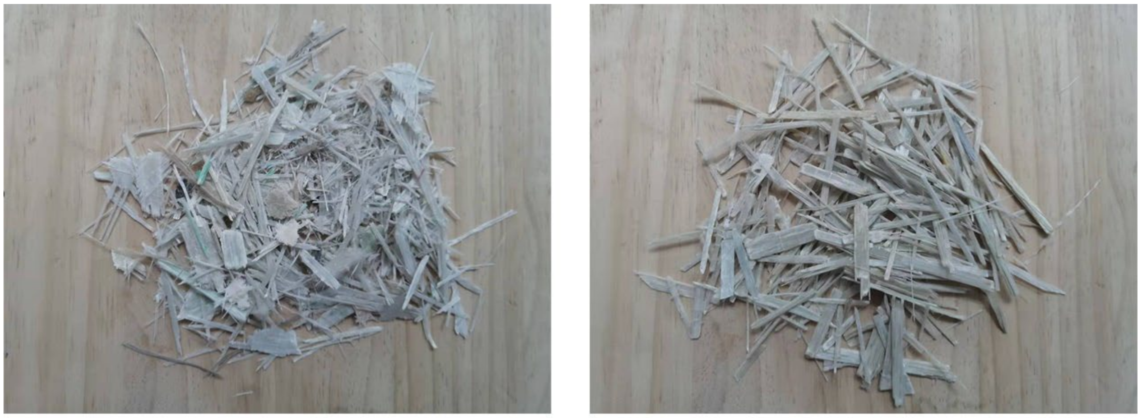

(a) GFRP waste (b) Selected macro fibers

Figure 3. A comparison of (a) the original GFRP waste; and (b) the selected macro fibers.

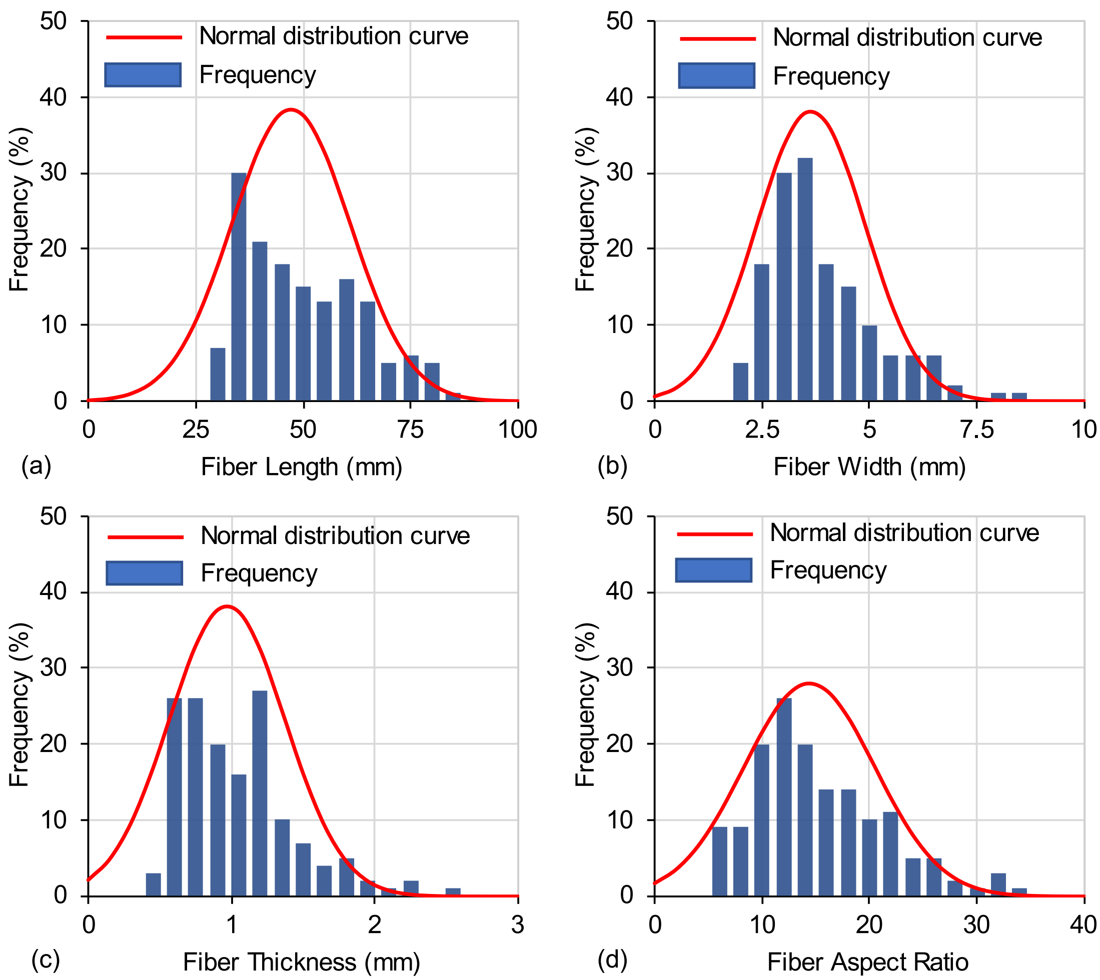

Figure 4. Statistical characteristics of recycled macro fiber dimensions: (a) length; (b) width; (c) thickness; and (d) aspect ratio.

Figure 5. Setup of flexural tests.

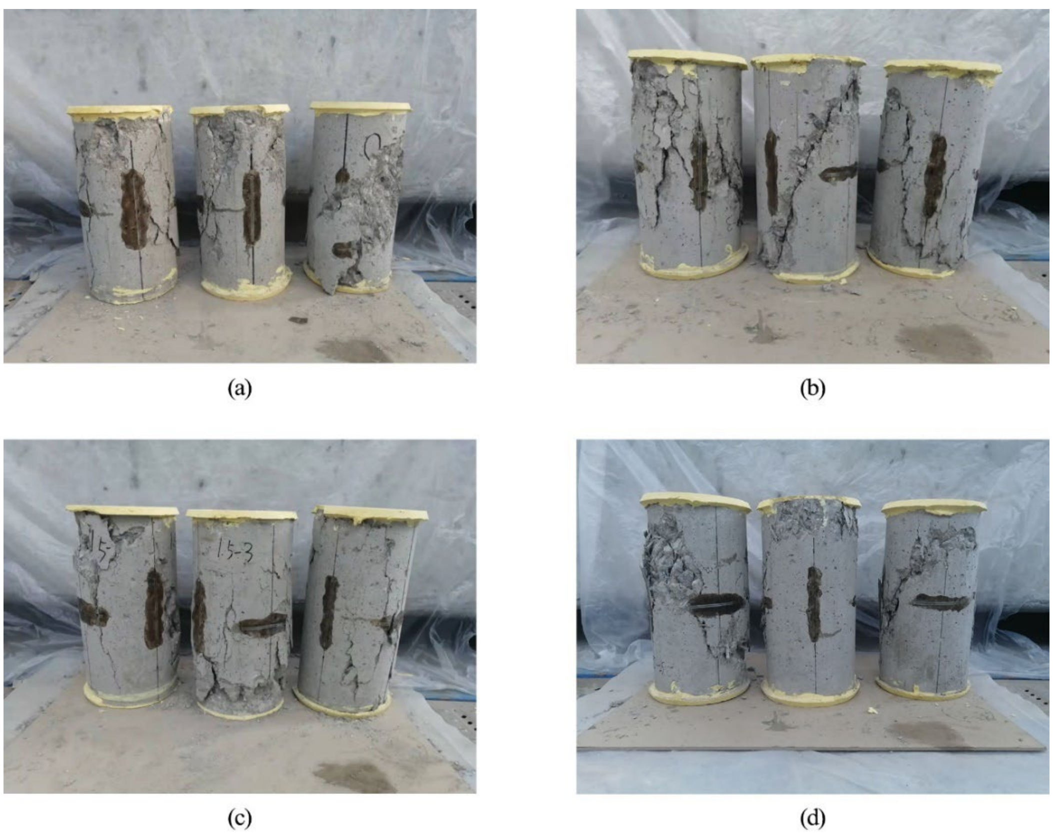

Figure 6. Failure patterns of Groups: (a) CC; (b) MFRC-0.5; (c) MFRC-1.5; and (d)MFRC-2.5 after compression tests.

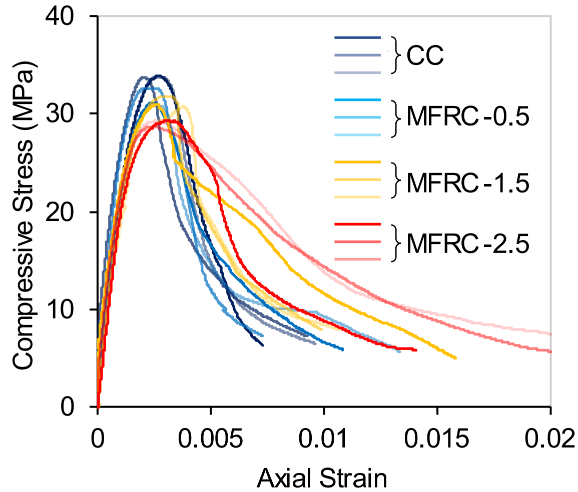

Figure 7. Compressive stress–strain curves of all groups.

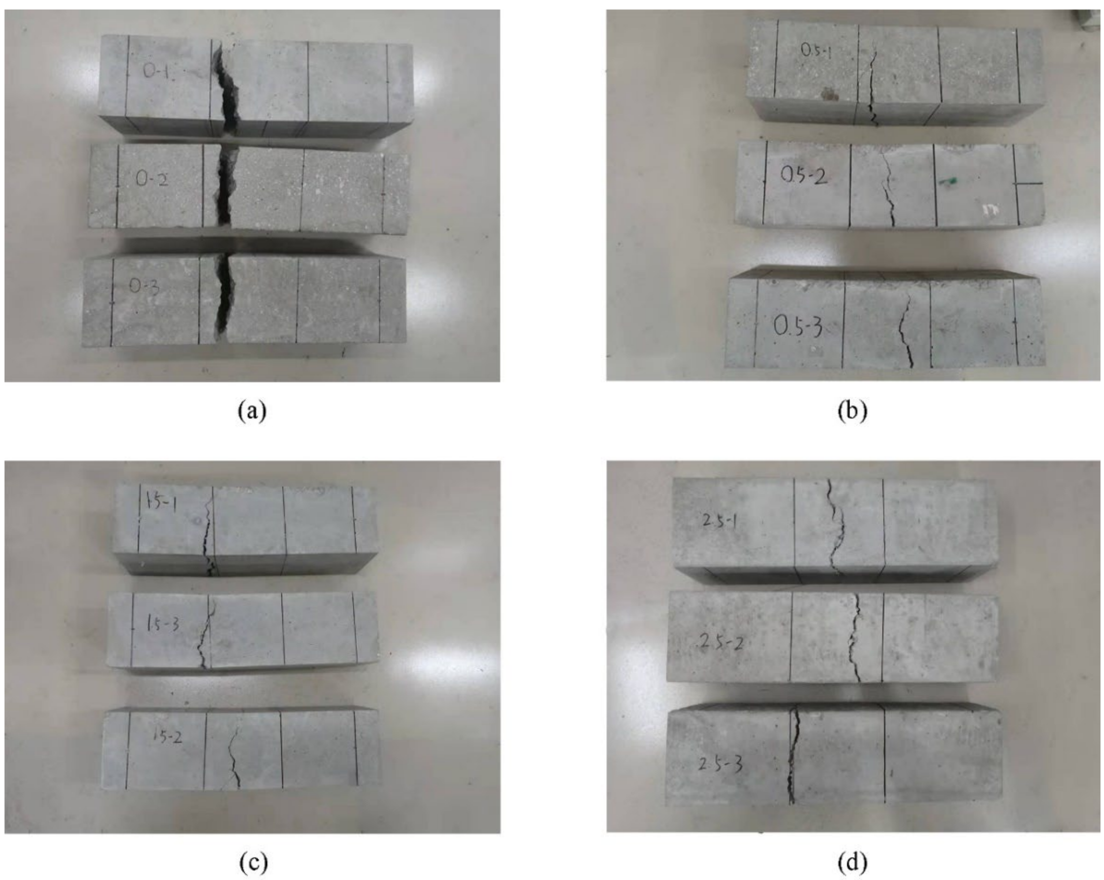

Figure 8. Failure patterns of Groups: (a) CC; (b) MFRC-0.5; (c) MFRC-1.5; and (d) MFRC-2.5 after flexural tests.

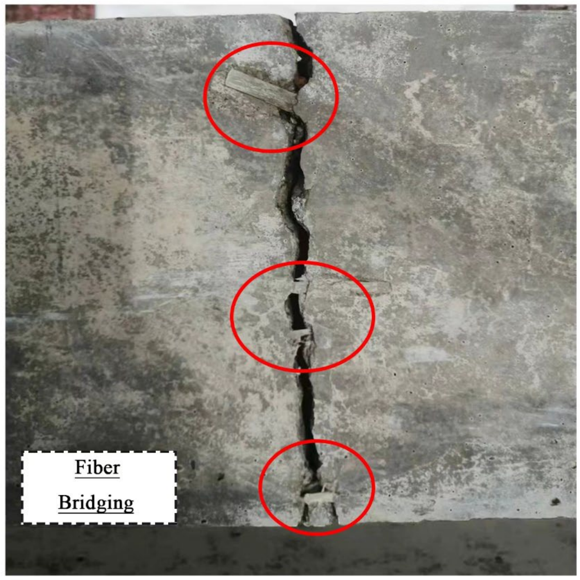

Figure 9. Fiber bridging at the bottom of concrete beams.

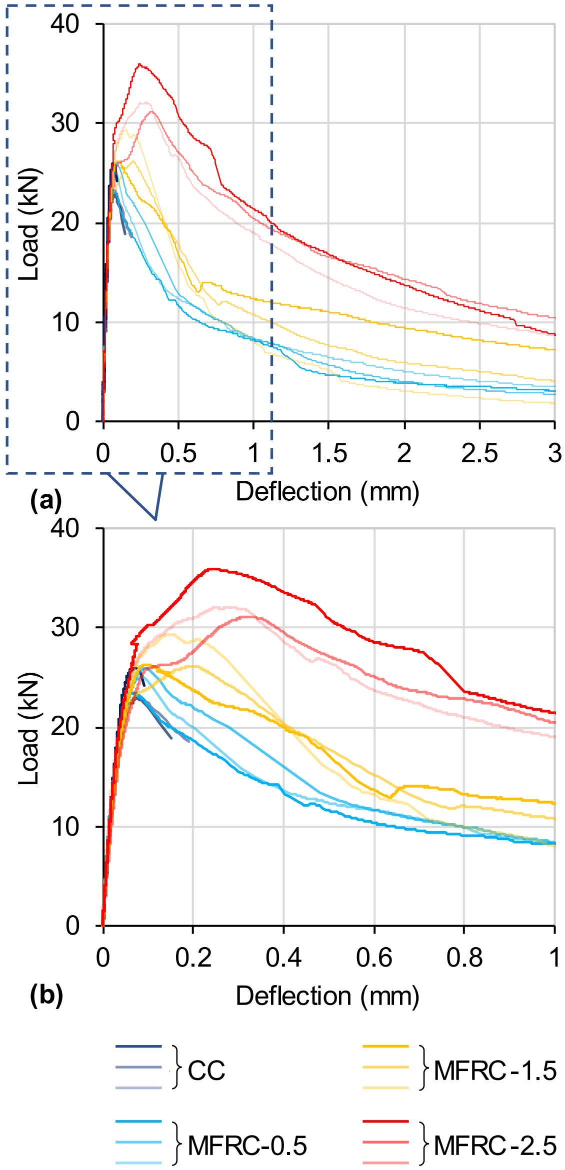

Figure 10. Flexural load-deflection curves for all groups: (a) the complete portions with deflection up to 3.5 mm; and (b) the initial portions with deflection up to 1.0 mm.

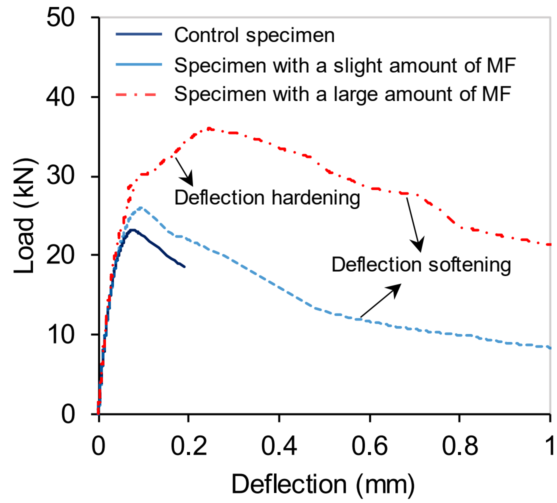

Figure 11. Three typical patterns of the flexural load-deflection curve.

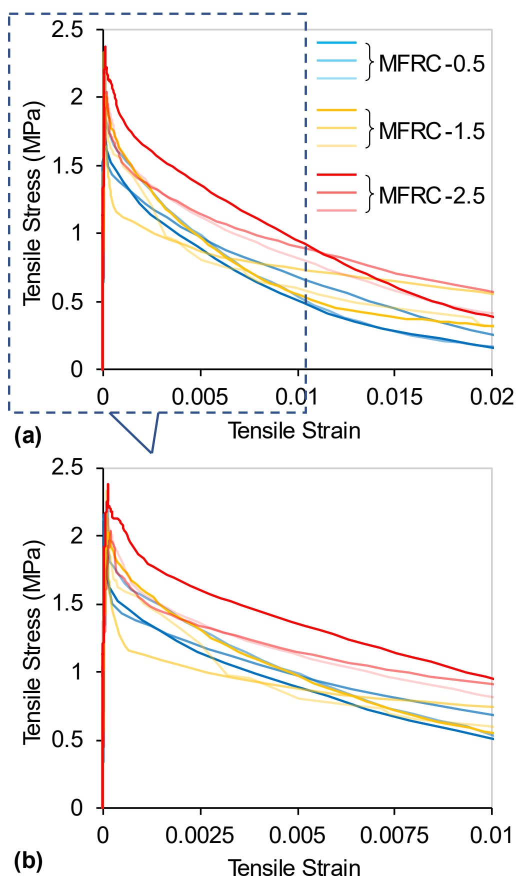

Figure 12. Tensile stress-strain curves obtained by inverse analyses: (a) the complete portions with deflection up to 3.5 mm; and (b) the initial portions with deflection up to 1.0 mm.